The EMBO Journal Vol.16 No.9 pp.2352–2364, 1997

Abnormal mesoderm patterning in mouse embryos mutant for the SH2 tyrosine phosphatase Shp-2

Tracy M.Saxton[1,2], Mark Henkemeyer[1,3], Stephan Gasca[2,4], Randy Shen[1,5], Derrick J.Rossi[1,3], Fouad Shalaby[4,6], Gen-Sheng Feng[1,7] and Tony Pawson[1,2,8]

[1]Programme in Molecular Biology and Cancer, Samuel Lunenfeld Research Institute, Mount Sinai Hospital, Toronto, Ontario M5G 1X5, [2]Department of Molecular and Medical Genetics, University of Toronto, Toronto, Ontario M5S 1A8, Canada, [4]Programme in Development and Fetal Health, Samuel Lunenfeld Research Institute Mount Sinai Hospital, Toronto, Ontario M5G 1X5, Canada and [7]Department of Biochemistry and Molecular Biology, Walther Oncology Center, Indiana University School of Medicine, Indianapolis, IN 46202, USA

[3]Present address: Center for Developmental Biology, University of Texas Southwestern Medical Center, Dallas, TX 75235, USA
[5]Present address: Department of Biochemistry and Molecular Biology, Walther Oncology Center, Indiana School of Medicine, Indianapolis, IN 46202, USA
[6]Present address: Department of Cardiovascular Molecular and Cellular Biology, Bristol Myers Squibb Pharmaceutical Research Institute, Lawrenceville, NJ 08543, USA

[8]Corresponding author

Shp-1, Shp-2 and corkscrew comprise a small family of cytoplasmic tyrosine phosphatases that possess two tandem SH2 domains. To investigate the biological functions of Shp-2, a targeted mutation has been introduced into the murine *Shp-2* gene, which results in an internal deletion of residues 46–110 in the N-terminal SH2 domain. Shp-2 is required for embryonic development, as mice homozygous for the mutant allele die *in utero* at mid-gestation. The *Shp-2* mutant embryos fail to gastrulate properly as evidenced by defects in the node, notochord and posterior elongation. Biochemical analysis of mutant cells indicates that Shp-2 can function as either a positive or negative regulator of MAP kinase activation, depending on the specific receptor pathway stimulated. In particular, Shp-2 is required for full and sustained activation of the MAP kinase pathway following stimulation with fibroblast growth factor (FGF), raising the possibility that the phenotype of Shp-2 mutant embryos results from a defect in FGF-receptor signalling. Thus, Shp-2 modulates tyrosine kinase signalling *in vivo* and is crucial for gastrulation during mammalian development.

Keywords: gastrulation/gene targeting/MAP kinase/Shp-2/tyrosine phosphatase

Introduction

Protein tyrosine kinases mediate the biological effects of a wide range of polypeptide growth factors. Tyrosine phosphorylation is reversed by tyrosine phosphatases, which comprise a large family of transmembrane and cytoplasmic enzymes (Sun and Tonks, 1994; Hunter, 1995). Such phosphatases can attenuate positive signals emanating from tyrosine kinases. Alternately, since tyrosine phosphorylation can be a negative regulator of signalling, as in the C-terminus of Src family kinases (Cooper and Howell, 1993), tyrosine phosphatases may also directly stimulate intracellular signalling by removing such inhibitory phosphorylation events.

A principal mechanism by which receptor tyrosine kinases (RTKs) stimulate downstream signalling pathways involves the recognition of phosphotyrosine sites on either the activated receptors or their substrates by the SH2 or PTB domains of cytoplasmic effector proteins (Cohen *et al.*, 1995; Pawson, 1995). A small family of SH2-containing tyrosine phosphatases may regulate signalling events immediately proximal to activated receptors for growth factors, cytokines and antigens. This group of phosphatases contains two vertebrate members, Shp-1 (previously termed Hcp, PTP1C, SH-PTP1, SHP; Adachi *et al.*, 1996) and Shp-2 (previously termed Syp, PTP1D, SH-PTP2, PTP2C; Freeman *et al.*, 1992; Ahmad *et al.*, 1993; Feng *et al.*, 1993; Vogel *et al.*, 1993), and *Drosophila* csw, a likely homolog of Shp-2 (Perkins *et al.*, 1992).

Genetic investigation of *csw* indicates that this phosphatase is a positive signal transducer downstream of the Torso RTK and is required for normal development of terminal structures in the *Drosophila* embryo (Perkins *et al.*, 1992). Through its SH2 domains, csw binds to activated Torso receptors and becomes tyrosine phosphorylated at its C-terminus (Cleghon *et al.*, 1996). *csw* has also been identified in a genetic screen for genes involved in photoreceptor cell development mediated by the sev RTK (Simon *et al.*, 1991). Wild-type (WT) csw is essential for R7 photoreceptor cell development, and a membrane targeted form of this phosphatase can drive R7 cell differentiation in the absence of sev (Allard *et al.*, 1996). csw does not bind directly to sev, but rather associates with an intermediate docking protein, dos (Herbst *et al.*, 1996; Raabe *et al.*, 1996).

The *Shp-1* gene is disrupted by the *motheaten* murine mutations (Shultz *et al.*, 1993; Tsui *et al.*, 1993), which cause excessive erythropoiesis, deregulated mast cell function and leukocyte hyperactivity. This genetic evidence for a negative regulatory role is complemented by several studies indicating that Shp-1 inhibits cell signalling mediated by interleukin-3, erythropoietin, steel factor, Fcγ and antigen receptors (Yi *et al.*, 1993; Cyster and Goodnow, 1995; D'Ambrosio *et al.*, 1995; Klingmuller *et al.*, 1995; Paulson *et al.*, 1996).

Shp-2 is widely expressed and becomes tyrosine phosphorylated after cell stimulation with a myriad of growth factors and cytokines (Feng *et al.*, 1993; Vogel *et al.*, 1993; Welham *et al.*, 1994). There is some contention

concerning the role of Shp-2 in tyrosine kinase signalling and the relative contributions of its SH2 domains, catalytic domain and C-terminal tail to its downstream effects (Milarski and Saltiel, 1994; Noguchi *et al.*, 1994; Rivard *et al.*, 1995; Tang *et al.*, 1995; Bennett *et al.*, 1996; Marengere *et al.*, 1996). Two tyrosine phosphorylation sites located at the C-terminus of Shp-2 are consensus binding sites for the SH2 domain of the Grb2 adaptor protein (YXNX; Bennett *et al.*, 1994; Songyang *et al.*, 1994). Thus, Shp-2 may be a positive effector of signal transduction by itself acting as an adaptor protein to link Grb2 and mSos1 to Ras, thereby leading to activation of the Raf/MAP kinase cascade (Bennett *et al.*, 1994; Li *et al.*, 1994; Noguchi *et al.*, 1994; Welham *et al.*, 1994). However, overexpression of Shp-2 protein in which the C-terminal tyrosines have been mutated to phenylalanine was shown to have no effect on MAP kinase activation or induction of DNA synthesis in response to growth factor stimulation (Bennett *et al.*, 1996). In contrast, overexpression of phosphatase-inactive mutants has suggested that Shp-2, but not Shp-1, plays a positive role in Ras/MAP kinase activation downstream of the receptors for epidermal growth factor, platelet derived growth factor (PDGF) and insulin. These experiments indicate that substrates specific for the Shp-2 catalytic domain may be essential for its positive role in signal transduction.

The N-terminal region of Shp-2 exerts an inhibitory effect on the catalytic activity of its phosphatase domain, which can be relieved by the binding of specific phosphopeptides to the SH2 domains (Lechleider *et al.*, 1993a; Pluskey *et al.*, 1995; Eck *et al.*, 1996; Pei *et al.*, 1996). Thus, the SH2 domains of Shp-2 may play a dual role in regulating its enzymatic activity and in directing the phosphatase to the proximity of its substrates. We have introduced a targeted mutation into the murine *Shp-2* gene which results in the deletion of 65 amino acids within the N-terminal SH2 domain. We find that WT Shp-2 is essential for embryonic survival and appears to play a key role during gastrulation in the organization of axial mesodermal structures and posterior development. Furthermore, we have used primary fibroblast-like cells isolated from mutant embryos to explore the role of Shp-2 in the regulation of MAP kinase activation elicited by fibroblast growth factors (FGFs) and to investigate the function of its SH2 domains in controlling signal transduction *in vivo*.

Results

Shp-2$^{\Delta 46–110}$ mutation

Clones of the *Shp-2* locus were obtained by screening an inbred 129/Sv strain mouse genomic library with a probe to the 5′ coding region of the Shp-2 cDNA (Feng *et al.*, 1993). To generate a mutation in the *Shp-2* locus, exon 3, encoding amino acids 46–110, was deleted by homologous recombination in embryonic stem (ES) cells and replaced by a neomycin resistance (neo^r) cassette (Figure 1A). Aggregation chimeras were generated and germline transmission of the mutant allele was obtained. Animals were routinely genotyped by Southern blot analysis (Figure 1B) or by *Shp-2*-specific PCR (Figure 1C). *Shp-2*+/– heterozygotes were long lived (>18 months) and fertile in 129 inbred, 129×CD1 hybrid and CD1 outbred backgrounds. However, no *Shp-2*–/– homozygous offspring were born following intercrosses between heterozygous males and females, indicating a recessive lethal phenotype (see below).

Since exons 2 and 4 are in-frame, it was possible that aberrant splicing around the inserted neo^r cassette could yield a mutant Shp-2 protein containing an internal deletion of residues 46–110, which comprise the majority of the N-terminal SH2 domain (SH2-N) and the short inter-SH2 region. To investigate the coding potential of the mutant allele, protein lysates of embryos isolated at 8.0 days of gestation (E8.0) were analyzed by Western blotting using either antibodies raised to the tandem SH2 domains (residues 2–216), or to the C-terminus (residues 576–593). Although the N-terminal antibodies did not recognize a polypeptide in the Shp-2–/– embryo lysates (Figure 1D), an abnormally sized gene product was observed when the C-terminal antibody was used (Figure 1E). In heterozygous specimens, the C-terminal antibody recognized both the WT 64 kDa and the Shp-2$^{\Delta 46–110}$ 57 kDa polypeptides. Densitometry indicated that the mutant protein is expressed at ~25% of WT levels, possibly due to inefficient splicing around the neo^r cassette.

To determine whether the transcript from the mutant *Shp-2$^{\Delta 46–110}$* allele was spliced to join exons 2 and 4, RT–PCR analysis of total RNA from heterozygous specimens was performed (Figure 1F and data not shown). PCR oligonucleotide primers flanking exon 3 amplified an internally deleted cDNA of the size expected. Sequencing confirmed the in-frame loss of codons for amino acids 46–110. Therefore, the mutant allele encodes a protein which retains the catalytic phosphatase domain and the C-terminal tail, but would be expected to be deficient in the binding of phosphotyrosine motifs as it lacks a functional SH2-N domain.

The Shp-2$^{\Delta 46–110}$ mutation is a recessive embryonic lethal

To characterize the lethality of homozygous mutant embryos, litters were dissected between E8.5 and E16.5 of development (Table I). No homozygous *Shp-2$^{\Delta 46–110}$* embryos were observed between E11.5 and E16.5, though visible resorbing dead embryos that could correspond to the mutant progeny class were detected. Homozygous *Shp-2$^{\Delta 46–110}$* mutant embryos could be detected at E10.5 of gestation, however, these embryos were necrotic (data not shown). The expected ratio (~25%) of *Shp-2$^{\Delta 46–110}$* homozygotes was observed at both E9.5 (27%) and E8.5 (20%) of development. These mutant embryos appeared viable, but their growth was retarded when compared with normal littermates and they exhibited severe developmental abnormalities (Figure 2). Examination of >100 different *Shp-2$^{\Delta 46–110}$* homozygotes at these stages revealed a variable phenotype. Approximately 70% of the mutants formed an identifiable anterior–posterior (A–P) axis, while the remaining 30% appeared more severely affected and had arrested development prior to the formation of recognizable embryonic structures (see below). Those forming a visible A–P axis appeared extremely abnormal. All had severe posterior truncations and had not initiated the process of turning. They also had few if any somites, disorganized neuroectoderm, abnormal formation of the midline structures and perturbed development of the

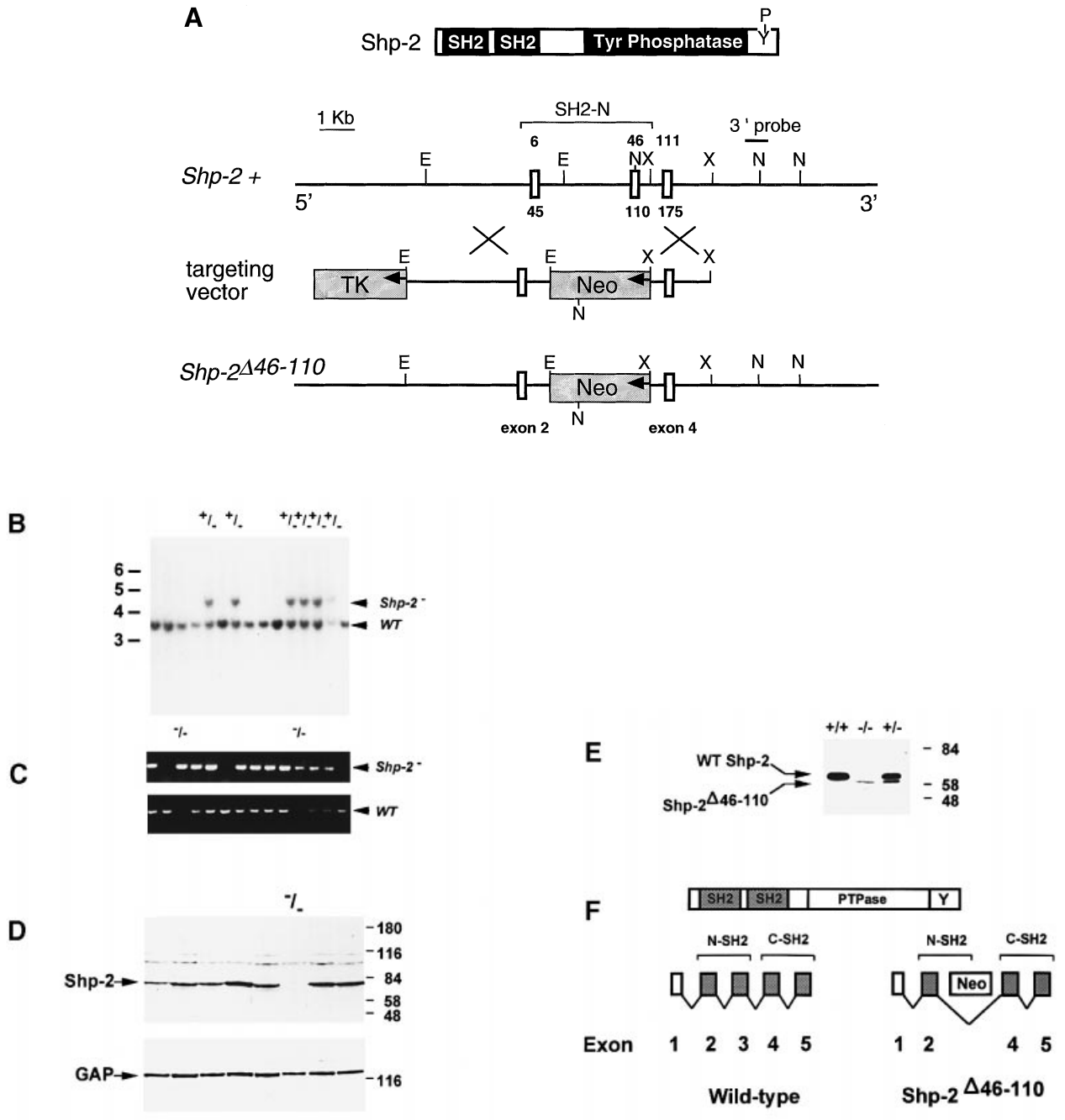

Fig. 1. Targeted mutation in *Shp-2*. (**A**) Protein structure, genomic locus and targeting strategy used to delete a 2.3 kb region of the *Shp-2* locus, including the exon encoding amino acids 46–110 of the SH2-N domain. Three exons (exons 2–4) of the WT murine *Shp-2* gene have been sequenced and are indicated by boxes. The external 3′ probe used to identify homologous recombination events is indicated above the WT restriction map. Only pertinent restriction sites are indicated and those below the DNA schematic are derived from vector sequences. N, *Nco*I; X, *Xho*I; E, *Eco*RI. (**B**) Southern blot analysis of genomic DNA digested with *Nco*I. Tail DNA isolated from weaned offspring of heterozygous intercrosses was subjected to Southern blot analysis using the external probe shown in (A). No homozygous mutant offspring were identified. (**C**) PCR analysis of the *Shp-2* mutation. Yolk sac DNA was obtained from heterozygous intercrosses collected at E9.0 and separate reactions were performed for the WT and mutant alleles. Two homozygous mutant offspring were identified. (D and E) Western blot analysis of embryo protein lysates. Embryos from heterozygous intercrosses were collected at E8.0. (**D**) Equal amounts of embryo lysate were subjected to Western blot analysis with both anti-Shp-2 SH2 (top panel) or, as a control, anti-GAP antibodies (lower panel). (**E**) Western blot analysis of cell lysates with anti-Shp-2 antibodies directed against the C-terminus of the protein. (**F**) Schematic of results of RT–PCR analysis and predicted splicing event generating the mutant mRNA transcript.

vasculature, including the heart and yolk sac (see Figure 2 and below).

Defective gastrulation in Shp-2 mutant embryos

Initial characterization of the *Shp-2*$^{\Delta 46–110}$ mutant phenotype indicated that the overall organization of the body plan was affected, consistent with a defect in gastrulation and embryonic patterning. During gastrulation, nascent mesodermal cells migrating out of the primitive streak differentiate into distinct cell types including those which form the axial, paraxial and lateral mesoderm. The overall organization of the embryonic body plan depends to a

considerable extent on the normal development of a specialized embryonic structure called the node, which in turn specifies cells forming the notochord, an axial mesoderm midline structure crucial for axis formation. To investigate whether the node or notochord were affected in the *Shp-2*$^{\Delta 46-110}$ homozygous embryos, the *cordon-bleu (cobl)–LacZ* transgene (Gasca *et al*., 1995) was employed to label axial mesoderm structures (Figure 3). In WT E8.5 specimens, *cobl* is expressed in the notochord, which runs the entire length of the embryo, from the midbrain to the tail bud (Figure 3A). In sharp contrast to WT embryos, *Shp-2*$^{\Delta 46-110}$ mutants isolated at E8.5 (Figure 3B) were abnormally small and had failed to elongate posteriorly and develop a notochord, appearing more similar in size to WT specimens isolated at E7.5 (Figure 3C). In WT E7.5 specimens, *cobl–LacZ* was solely expressed in the node and in a few mid-line cells anterior to the node. The node-like structure in the E8.5 *Shp-2*$^{\Delta 46-110}$ mutants appeared larger than in WT E7.5 specimens, indicating that cells may have accumulated at this structure, perhaps from a failure to differentiate and/or migrate properly. The intensity of *cobl–LacZ* staining at E8.5 was variable between different *Shp-2*$^{\Delta 46-110}$ mutants. In the extreme situation, some embryos did not express any *cobl–LacZ*, nor did they form a distinguishable node (data not shown).

E9.5 *Shp-2*$^{\Delta 46-110}$ mutant embryos were identified and stained for *cobl–LacZ* (Figure 3D). Although these mutant embryos had developed a defined A–P axis, all exhibited

Table I. Genotype analysis of the progeny from Shp-2+/– intercrosses

	Normal		Mutant
	+/+	+/–	–/–
Adult	86 (39%)	135 (61%)	0
E16.5	10[a]		0 [1]
E14.5	10[a]		0 [2]
E11.5	24[a]		0 [7]
E10.5	3	10	3[b,c]
E 9.5	35 (28%)	55 (45%)	33[b] (27%)
E 8.5	9 (26%)	19 (54%)	7[b] (20%)

[ ] indicates resorption.
[a] Genotype not determined.
[b] These embryos were abnormal in appearance.
[c] These embryos were highly necrotic.

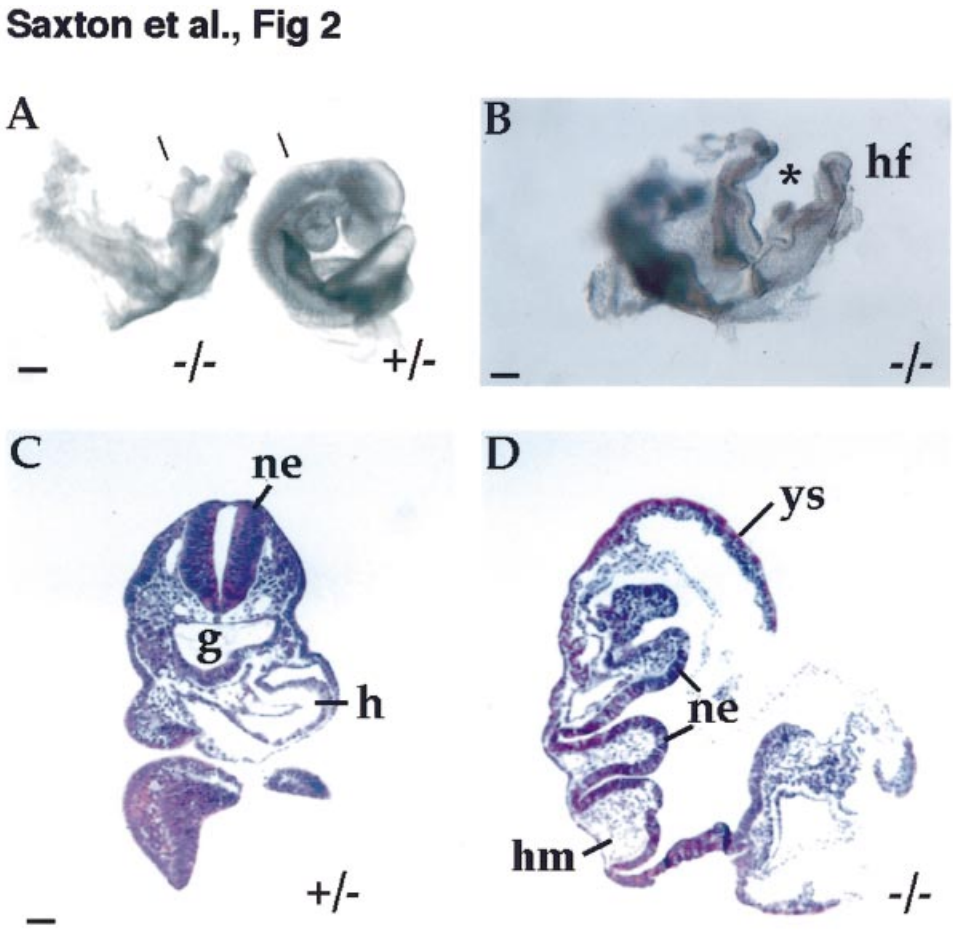

Fig. 2. *Shp-2*$^{\Delta 46-110}$ mutant embryos exhibit severe developmental abnormalities. (A and B) Whole mount of a *Shp-2*$^{\Delta 46-110}$ homozygous mutant embryo compared with a heterozygous littermate isolated at E9.0. Dorsal is up and anterior is to the right. (**A**) The *Shp-2*$^{\Delta 46-110}$ mutant embryo is smaller, poorly organized, has failed to turn and somites have not developed. (**B**) A dorsal view looking down the midline of the same mutant embryo shown in (A). The headfolds (hf) are abnormal and are not fused at the midline (*). (C and D) Sections of heterozygous (**C**) and homozygous mutant (**D**) embryos. Planes of sections are indicated by a bar on (A). The neuroectoderm (ne) and head mesenchyme (hm) of the *Shp-2*$^{\Delta 46-110}$ mutant embryo is malformed. Most of the structures identifiable in the heterozygous embryo could not be identified in the mutant embryo. Gut, g; heart, h; yolk sac, ys. Scale bars: A, 200 μm; B, 100 μm; C and D, 50 μm.

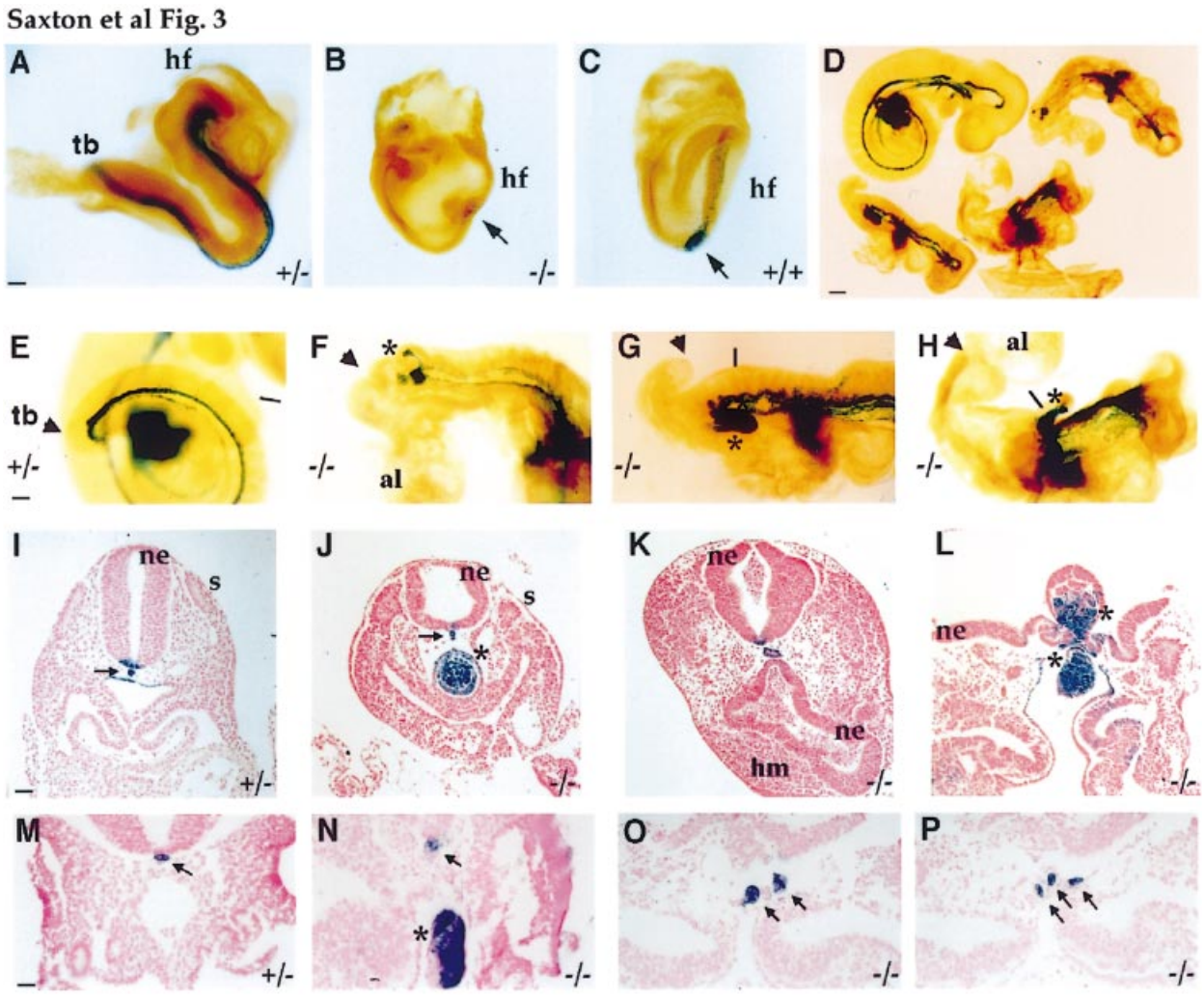

Fig. 3. Defective mesoderm patterning in homozygous *Shp-2*$^{\Delta 46-110}$ embryos. (A–L) Embryos containing the *cobl–LacZ* marker were collected between E8.5 and E9.5 of development, stained for β-gal activity and viewed as whole-mount specimens (**A**–**H**) or as tissue sections (**I**–**L**). Dorsal is up and anterior is to the right. (A–C) *Shp-2*$^{\Delta 46-110}$ heterozygous (A) and homozygous (B) littermates collected at E8.5 of development. *cobl–LacZ* expression is confined to the notochord, floor plate of the neural tube and the roof of the gut. The notochord, which can be clearly seen in the heterozygous embryo as the ribbon of blue-staining cells running the A–P length of the embryo to the chordoneural hinge at the tail bud (tb), has failed to develop in the *Shp-2*$^{\Delta 46-110}$ mutant embryo. As E8.5 mutant embryos seem delayed in development, for comparison, an E7.5 WT embryo is shown (C). Arrows in (B) and (C) point to the presumptive node; this organization site of the mutant embryo failed to develop normally as indicated by the reduced β-gal staining. (D) E9.5 embryos stained for the *cobl–LacZ* marker. A *Shp-2*$^{\Delta 46-110}$ heterozygote is shown in the top left and the other three embryos are homozygous mutants. (E–H) Higher magnification of the posterior region of the embryos shown in (D). The posterior end of each embryo is marked by an arrowhead. The *Shp-2*$^{\Delta 46-110}$ heterozygote (E) shows a thin line of blue staining notochord cells. *Shp-2*$^{\Delta 46-110}$ mutant embryos (F–H) do not extend a labelled notochord to the posterior tip of the tail. In the mutant embryos, abnormal accumulations of *cobl*-expressing cells were identified which form aberrant secondary extentions of the notochord into one or two more additional branches (* in F–H).
(I–L) Transverse sections through mid-body (I, J and L) or the anterior region (K) of E9.5 embryos stained for *cobl–LacZ* expression. The plane of section for (I) is shown in (E), (J) is shown in (G), (L) is shown in (H) and (K) is not shown, but is through the anterior of the embryo in (G). In WT or heterozygous (I) embryos stained for *cobl–LacZ*, the notochord is comprised of a small group of blue staining cells (arrow) just ventral of the neural tube at the midline. The *Shp-2*$^{\Delta 46-110}$ mutant embryo shown in (J) exhibits a relatively normal notochord (arrow) but also possesses an abnormal mass of *cobl–LacZ* staining cells protruding into the gut of the embryo (*). An anterior section of this same embryo (K) shows that the head mesenchyme (hm) and neuroectoderm (ne) is irregularly formed and the neural tube is filled with cellular material. The neuroectoderm of the embryo shown in (L) has failed to close to form a neural tube and the *cobl*-expressing domain is grossly abnormal. One of the ectopic *cobl*-stained projections (*) runs through the gut of the embryo (ventral projection) and a second is noted above the neuroectoderm (dorsal projection). Somite formation (s) is impaired (J) or absent (L) in the mutant embryos as compared with heterozygous embryos (I). (**M**–**P**) Transverse sections through mid-body of E9.5 heterozygous (M) or *Shp-2*$^{\Delta 46-110}$ homozygous (N-P) embryos probed for expression of mRNA for the axial mesoderm marker *T*. Arrows point to notochord(s), the (*) indicates abnormal projection of *T* expressing cells through the gut of the embryo (N). (O) and (P) are sections of the same embryo which exhibited a split notochord, (O) being more anterior than (P). Scale bars: A–C, 150 μm; D, 400 μm; E–H, 100 μm; I–L, 50 μm; M–P, 30 μm.

varying degrees of posterior truncations that were associated with abnormalities in the development of the node/tail bud and the notochord. By E9.5, WT and heterozygous embryos had formed 20–24 pairs of somites and had a smoothly curving notochord which expressed *cobl–LacZ* from the midbrain to the chordoneural hinge at the posterior tip of the tail (Figure 3E). Some *Shp-2*$^{\Delta 46-110}$ mutants were able to form somites (Figure 3F and G), whereas others failed to make any recognizable somites (Figure 3H). All three of the mutant embryos exhibited

an abnormal notochord, as highlighted by the pattern of *cobl–LacZ* expression. The well developed *Shp-2*$^{\Delta 46–110}$ mutant embryo shown in Figure 3F had a relatively normal notochord that almost reached the posterior tip of the tail. However, at the posterior tip of this embryo, there was a buildup of *cobl–LacZ* expressing cells, from which there were several abnormal projections of notochord-like material (* in Figure 3F–H). In a more severely affected *Shp-2*$^{\Delta 46–110}$ mutant embryo, the neural tube and the notochord were kinked and *cobl–LacZ* expression did not extend to the posterior tip of the embryo (Figure 3G). Instead, a large mass of *cobl*-positive cells extending anteriorly from the most posterior extent of the notochord was present. An even more defective mutant (Figure 3H) exhibited a dramatic posterior truncation of the notochord. This embryo also had an expansion of *cobl–LacZ* expressing cells and displayed an abnormal structure of labelled cells that projected outside of the embryo on its dorsal surface.

Transverse sections highlight the defects observed in the *Shp-2*$^{\Delta 46–110}$ mutant embryos. In WT E9.5 sections, *cobl–LacZ* was expressed in cells corresponding to the notochord, the floorplate of the neural tube and the roof of the gut (Figure 3I). In the moderately well developed mutants, *cobl–LacZ* expression labelled the notochord; however, additional labelled cells were also identified (Figure 3J–L). Instead of labelling a small group of cells at the midline, *cobl–LacZ* expression in mutant embryos was frequently expanded and observed to accumulate and protrude within the gut of the embryos.

To confirm that these abnormal tissues corresponded to axial mesoderm structures, an independent marker for the node and the notochord was analyzed. The *Brachyury* (*T*) gene is solely expressed within axial mesoderm (Wilkinson *et al.*, 1990) and therefore should directly highlight defects in the development of this tissue. Whole-mount RNA *in situ* hybridization studies were performed on *Shp-2*$^{\Delta 46–110}$ mutants using a *T* probe. This analysis corroborated the results obtained with *cobl* (Figure 3M–P). Of particular significance was the identification in E9.5 mutants of accumulations of *T*-positive cells protruding into the gut (Figure 3N) and of multiple or split notochords (Figure 3O and P). Furthermore, at E8.5 some mutant embryos did not stain for *T* at all and others stained an abnormal or delayed primitive streak, which is reminiscent of expression observed for WT E7.0 embryos (data not shown).

The combined results of *cobl* and *T* expression indicate that the development of axial mesodermal structures are severely affected in *Shp-2* mutant embryos. One possible outcome of an inability to properly gastrulate would be a phenotype in which the embryos are so severely affected that they fail to form an A–P axis. Indeed, we found that ~30% of the *Shp-2* homozygotes failed to develop an A–P axis, or any recognizable embryonic structures at all (Figure 4). These embryos were observed between E7.5 and 10.5 of development and expressed a wide array of markers for different cell types, including *cobl–LacZ* (Figure 4A), an endothelial marker *Flk1–LacZ* (Figure 4B and see below; Shalaby *et al.*, 1995) and a marker mainly restricted to the developing nervous system, *Nuk–LacZ* (Figure 4C and D; Henkemeyer *et al.*, 1996). These severely affected embryos may represent the class of *Shp-2*$^{\Delta 46–110}$ mutants which failed to develop a node, as observed in several E8.5 embryos which did not stain for *cobl–LacZ* or *T* expression. The failure of some *Shp-2*$^{\Delta 46–110}$ embryos to develop any axis indicates a crucial role in early gastrulation for Shp-2, which can be overcome to some degree by many of the *Shp-2*$^{\Delta 46–110}$ mutant embryos, potentially due to the retention of partial function of the Shp-2$^{\Delta 46–110}$ protein.

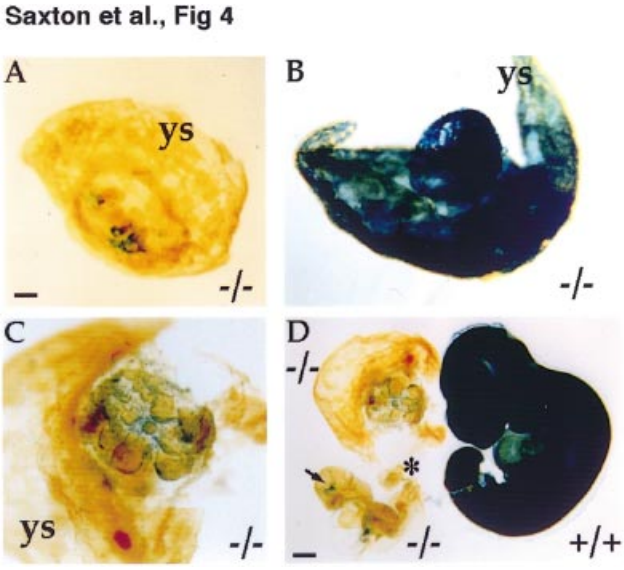

Fig. 4. A subset of *Shp-2* homozygotes do not form an A–P axis. (A–C) *Shp-2*$^{\Delta 46–110}$ mutant embryos dissected at E9.5 (A and B) and E10.5 (C) that have failed to develop an A–P axis, or any recognizable embryonic structures, yet still retain the expression of many tissue-specific markers. (**A**) *cobl–LacZ*; (**B**) *Flk1–LacZ* (endothelial marker); (**C**) *Nuk–LacZ* (neural marker). The yolk sac (ys) is indicated for each embryo. (**D**) E10.5 littermates stained for *Nuk–LacZ* expression. The highest level of *Nuk–LacZ* expression is in the ventral hindbrain, and the fidelity of this expression is kept for the E10.5 *Shp-2*$^{\Delta 46–110}$ mutant embryo that developed an A–P axis (bottom left, arrow). This mutant embryo, even by E10.5 of development, has failed to turn. Note that the WT littermate was stained for the same period of time, indicating a much reduced level of *Nuk–LacZ* expression in the *Shp-2* mutants. The inability to form an A–P axis was not due to the maternal environment of these embryos, as both classes of mutant embryos could be detected in the same litter. Scale bars: A–C, 200 μm; D, 400 μm.

Vascular defects in Shp-2 mutants

Upon dissection of mutant embryos, we noted that the yolk sac appeared abnormally thin and wrinkled. We used *Flk1–LacZ* as a marker to label endothelial cells in *Shp-2*$^{\Delta 46–110}$ mutants (Figure 5). By E9.5, embryos stained for *Flk1–LacZ* expression showed a complex network of blood vessels throughout the embryo, which was also present in mutant embryos (Figure 5A and B), demonstrating their ability to form a network of endothelial cells. *Flk1-LacZ* expression in E9.5 yolk sacs of mutant embryos indicated that *in situ* vasculogenesis and the production of the primary capillary plexus occurred normally. However, the yolk sac blood vessels failed to re-organize into a highly vascularized network in the mutants (Figure 5C and D) and remained in the honeycombed pattern reminiscent of E8.5 WT embryos.

Transverse sections of these embryos confirmed the presence of a vascular network within the mutants (Figure

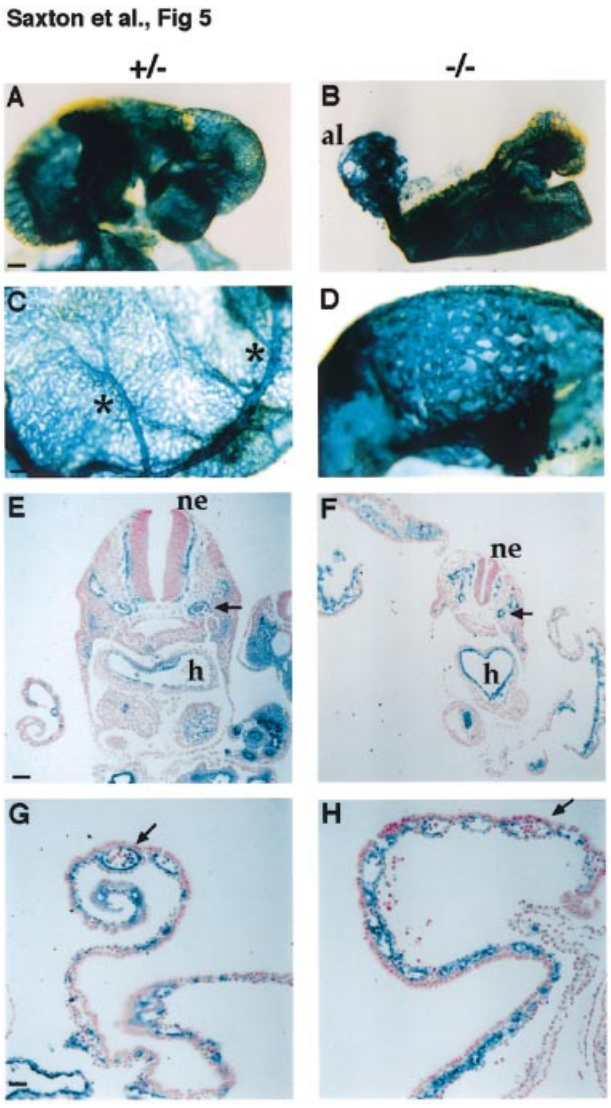

Fig. 5. Expression of the mesodermal marker *Flk1–LacZ*. (A–D) Whole mounts of E9.5 embryos (**A** and **B**) and yolk sacs (**C** and **D**) stained for the expression of the endothelial marker *Flk1–LacZ*. Embryos heterozygous (A and C) and homozygous (B and D) for the mutation developed an extensive vascular network. The mutant embryo has not turned and the allantoic mesoderm (al) has not fused with the maternal circulation. The endothelial cells in the mutant yolk sac formed the primary capillary plexus, however, they do not remodel into the highly vascularized network seen in heterozygous littermates (* in C). (E and F) Transverse sections through mid-body of a *Shp-2*$^{\Delta 46–110}$ heterozygote (**E**) and a homozygous mutant embryo (**F**) demonstrates the ability of mutant embryos to develop normal dorsal aortae (arrows in E and F), although the heart (h) does not form normally in the mutant embryo. (G and H) Sections through heterozygote (**G**) or mutant (**H**) yolk sacs at E9.5 of development. Both specimens formed endothelial cell lined blood vessels that contain primitive haematopoietic cells (arrows). Scale bar A and B, 150 μm; C–F, 100 μm; G and H, 50 μm.

5E and F). Even though the heart formed somewhat abnormally, it was often beating at the time of dissection. Sections through the yolk sac (Figure 5G and H) showed that blood vessels did form within the mutant yolk sac and that primitive blood cells were present. However, thick-walled blood vessels, which are the main arteries and veins delivering nutrients to the embryo, did not form in the mutant yolk sacs. The allantois (Figures 5B, 3F and H) did not develop properly nor connect to the placenta, leading to death and resorption of these embryos by E10.0–11.0 of gestation. These studies indicate that WT Shp-2 protein is not required for endothelial differentiation, but rather is needed for certain aspects of vascular endothelial cell organization.

Shp-2 is required for RTK signalling

The phenotypes observed in the *Shp-2*$^{\Delta 46–110}$ mutant embryos are likely due to a deregulation of tyrosine kinase signalling during development. To address whether the Shp-2$^{\Delta 46–110}$ protein could function downstream of activated growth factor receptors, primary cell cultures from homozygous mutant, heterozygous and WT embryos were established. In order to test biochemically the binding properties of the Shp-2$^{\Delta 46–110}$ protein, we analyzed its interactions with the β receptor for PDGF (PDGFR), as both the SH2-N and the SH2-C domains of Shp-2 bind to the activated form of this growth factor receptor (Lechleider *et al.*, 1993b; Case *et al.*, 1994; Feng *et al.*, 1994). Cultures were stimulated with PDGF, Shp-2 proteins were immunoprecipitated with the C-terminal antibody and precipitates were probed with either anti-phosphotyrosine or anti-Shp-2 antibodies (Figure 6A). Upon addition of PDGF, both the WT and mutant forms of Shp-2 became tyrosine phosphorylated. This result, however, does not indicate that Shp-2$^{\Delta 46–110}$ can still bind to the PDGFR, as a mutant form of the receptor (Y1009F) that can no longer associate with Shp-2 still induces tyrosine phosphorylation of this protein (Kazlauskas *et al.*, 1993). Indeed, we found that although autophosphorylated PDGFR was present in anti-Shp-2 precipitates from WT or heterozygous cells, the activated receptor could not be detected in association with the Shp-2$^{\Delta 46–110}$ protein (Figure 6A). Consistent with this observation, a GST fusion protein containing both Shp-2 SH2 domains bound *in vitro* to the activated PDGFR, while the corresponding mutant protein lacking residues 46–110 did not (Figure 6B). These results suggest that the Shp-2$^{\Delta 46–110}$ protein is impaired in its ability to bind the autophosphorylated PDGFR.

Shp-2 has been implicated in the activation of MAP kinase, which serves as a downstream effector of Ras proteins. To assess whether MAP kinase becomes activated by the PDGFR in the absence of WT Shp-2 protein, gel shift assays, which correlate directly with the activation of this enzyme, were performed. An enhanced and potentiated MAP kinase activation in response to PDGF stimulation was observed in the *Shp-2*$^{\Delta 46–110}$ cells as compared with WT cells (Figure 7A). At 5 min post-stimulation, 98% of MAP kinase was in the phosphorylated active state in the mutant cells, whereas only 67% of MAP kinase was activated in WT cells (Figure 7C, left graph). Similarly, at 80 min after addition of PDGF, 32% of MAP kinase remained activated in mutant cells, as compared with 20% in WT cells. These results show that Shp-2 protein is involved in regulating the intensity of MAP kinase activation during PDGF signalling.

Mutation within the murine PDGFRs induce embryonic phenotypes which effect later stages of murine development than that exhibited by *Shp-2* mutant embryos. This suggests that the *Shp-2* mutant phenotype results from dysregulation of growth factor receptor pathways important earlier in development than the PDGFR pathways.

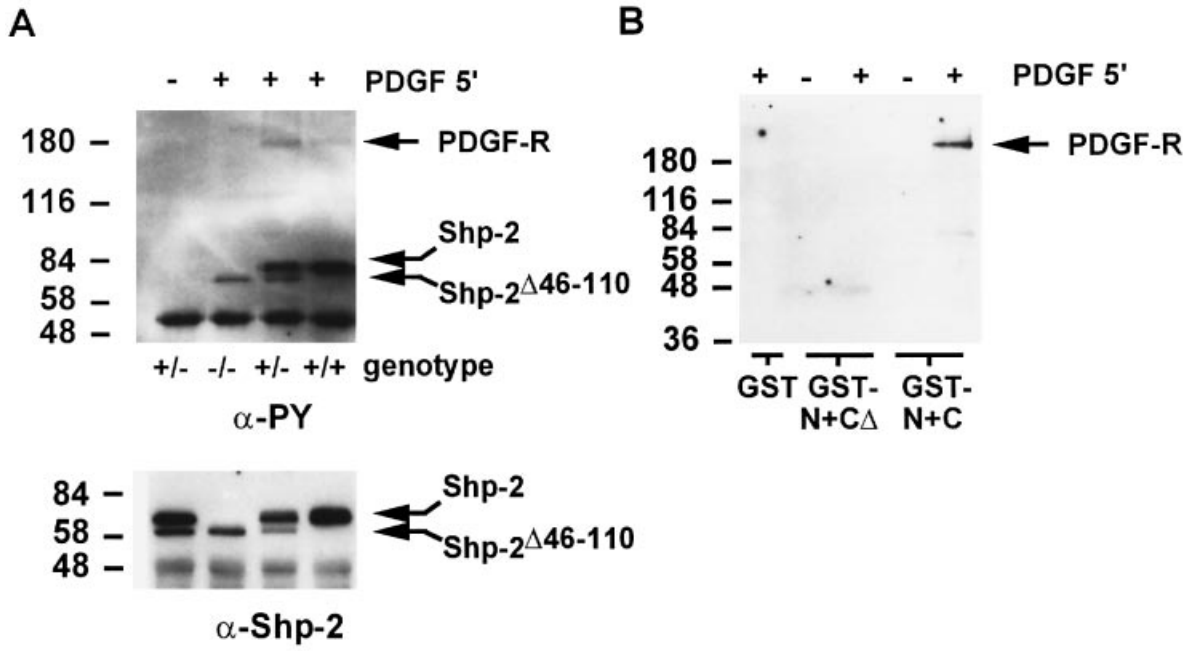

Fig. 6. Shp-$2^{\Delta 46–110}$ protein does not associate with activated PDGFR. (**A**) Shp-$2^{\Delta 46–110}$ becomes tyrosine phosphorylated upon stimulation of homozygous mutant or heterozygous cells with PDGF. Quiescent cells were either left unstimulated (–) or stimulated for 5 min (+). 100 μg of the corresponding lysates were immunoprecipitated with the anti-Shp-2 C-terminal antibody and probed with anti-phosphotyrosine (top panel) or anti-Shp-2 antibodies (bottom panel). (**B**) The *Shp-*$2^{\Delta 46–110}$ mutation prevents binding of Shp-2 SH2 domains to the activated PDGFR. Lysates from NIH 3T3 cells unstimulated (–) or stimulated with PDGF (+) were incubated with GST, GST-$NC^{\Delta 46–110}$ (N+CΔ) or GST-N+C. Precipitated proteins were detected using anti-phosphotyrosine antibodies.

FGFs have been implicated in controlling numerous developmental decisions, including those made during gastrulation. Furthermore, disruption of the *Fgf-R1* gene by homologous recombination (Yamaguchi *et al.*, 1994; Deng *et al.*, 1994) leads to a recessive lethal phenotype that is similar to, though distinct from, the *Shp-*$2^{\Delta 46–110}$ mutant phenotype described here (see Discussion). In addition, activation of MAP kinase is known to be crucial for the induction of mesoderm by FGF (Gotoh *et al.*, 1995; Labonne *et al.*, 1995; Umbhauer *et al.*, 1995). RT–PCR analysis from total RNA isolated from primary cells indicated that the *Fgf-R1* gene was expressed in the primary cell cultures from both WT and mutant embryos (data not shown). To address whether the Shp-2 protein is involved in signalling downstream of FGF receptors, WT and mutant primary cultures were subjected to a time course of FGF stimulation followed by analysis of MAP kinase mobility. The MAP kinase gel shift of the *Shp-*$2^{\Delta 46–110}$ mutant cells in response to FGF was greatly reduced and transient in comparison with WT cells (Figure 7B). Densitometry analysis indicated that at 5 min after addition of FGF to the WT cells, ~70% of MAP kinase was shifted, compared with only 17% in the mutant cells (Figure 7C, right graph). Maximal MAP kinase activation of both WT (80% shifted) and mutant (57% shifted) cells was observed within 10 min of FGF stimulation. WT and mutant cells also showed a sharp distinction in their ability to achieve a sustained level of MAP kinase activation following FGF stimulation. In WT cells, 70% of the MAP kinase remained in the activated state 80 min after FGF stimulation. In contrast, only 5% of MAP kinase was phosphorylated in the mutant cells at this time. These results indicate that Shp-2 is required in a positive fashion for robust and sustained activation of MAP kinase by FGF, consistent with the supposition that Shp-2 and FGF receptors act in the same signalling pathway during gastrulation.

Discussion

We describe effects on murine embryonic development and MAP kinase activation resulting from a mutation in the gene encoding the Shp-2 SH2 domain-containing tyrosine phosphatase. In the absence of WT Shp-2 protein, the production of axial mesoderm is severely perturbed as indicated by abnormalities in the node, notochord and the A–P axis. These embryos also exhibit poorly developed somites and kinked or unclosed neural tubes. Extra-embryonic mesoderm also requires functional Shp-2 protein, as endothelial cells within the yolk sac of *Shp-2* mutants remain in the primitive honeycombed pattern rather than re-organizing into a highly vascularized network. Finally, the allantoic mesoderm is underdeveloped and fails to fuse with the maternal circulation, leading to the death and resorption of these mutant embryos between E10 and 11.0 of gestation. Tyrosine kinase receptors, such as those for the FGF family, are known to function in the process of mesoderm induction. We show that the *Shp-*$2^{\Delta 46–110}$ mutation leads to a failure of cells to fully activate MAP kinase in response to FGF. Moreover, in WT cells, FGF led to an extended duration of MAP kinase activation which lasted >80 min, whereas in *Shp-2* mutant cells only a transient peak of MAP kinase activation was observed which was rapidly down-regulated to near basal levels. Interestingly, not all tyrosine kinase receptors require Shp-2 to fully activate MAP kinase, as stimulation of the same *Shp-*$2^{\Delta 46–110}$ mutant cell cultures with PDGF hyper-activated signalling through this receptor leading to

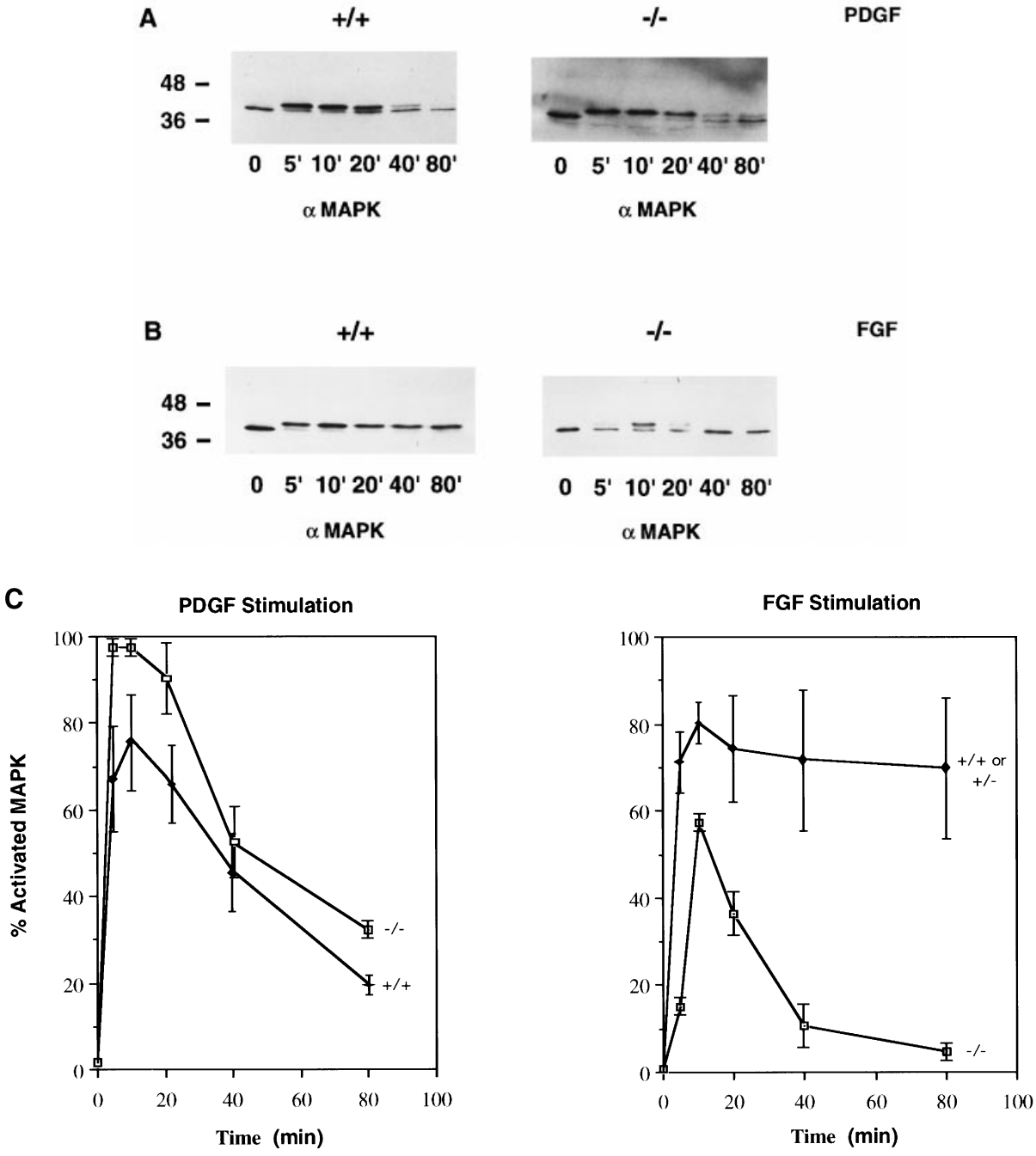

Fig. 7. Homozygous *Shp-2*$^{\Delta 46–110}$ fibroblasts elicit differential MAP kinase activation in response to PDGF and FGF. (**A**) MAP kinase gel shift assay comparing the response of WT (left panel) and mutant (right panel) embryo fibroblasts to addition of PDGF. Times following PDGF stimulation are indicated. Activated MAP kinase exhibits a reduced mobility in these assays. (**B**) MAP kinase gel shift assay comparing the WT (left panel) to mutant (right panel) fibroblasts response to FGF stimulation. (**C**) Comparison of MAP kinase mobility change in response to PDGF versus FGF. Densitometry of anti-MAP kinase immunoblots from ⩾3 experiments was performed to obtain a ratio of phosphorylated (activated) to unphosphorylated MAP kinase. The results for cells stimulated with PDGF (left graph) are compared with cells stimulated with FGFs (right graph). The large standard deviation in MAP kinase phosphorylation state observed for FGF stimulation for non-mutant cells may result from combining results obtained from both +/+ and +/– cells. The +/– cells may have a reduced ability to activate MAP kinase following FGF stimulations compared with the +/+ cells (data not shown).

heightened MAP kinase activation. Our results suggest that Shp-2 plays a critical role in controlling tyrosine kinase signalling in the mouse embryo.

The Shp-2$^{\Delta 46–110}$ *allele*

The *Shp-2*$^{\Delta 46–110}$ mutant allele encodes a 57 kDa protein, which is expressed at ~25% of wild type Shp-2 protein levels and results from in-frame splicing around the inserted neo^{r} cassette. The Shp-2$^{\Delta 46–110}$ protein lacks residues responsible for phosphopeptide recognition by the SH2-N domain (Lee *et al.*, 1994), as well as the inter-SH2 region, which forms part of the hydrophobic core that orients the tandem SH2 domains (Eck *et al.*, 1996). Deletion of residues 46–110 in the N-terminal SH2 domain

would be expected to entirely destroy the phosphotyrosine binding properties of the SH2-N domain, and might also influence the activity of the C-terminal SH2 domain. Indeed, we show that disruption of this region severely compromises the ability of Shp-2 to bind the PDGFR.

The *Shp-2*$^{\Delta 46–110}$ mutation is not a dominant inhibitory allele of *Shp-2*, as heterozygous animals have no obvious phenotype, while homozygotes have a striking embryonic defect. While we cannot rule out the possibility that *Shp-2*$^{\Delta 46–110}$ is a hypomorphic allele, it is clear that the mutation induces a severe phenotype, and may be tantamount to a genetic null. Indeed, it is interesting to note that a protein null mutation within the *Shp-2* gene leads to resorption of the homozygous mutant embryos at the same time of gestation as the *Shp-2*$^{\Delta 46–110}$ allele (Arrandale *et al.*, 1996). Although the embryonic phenotype of the protein null mutation has not been analyzed, these results suggest that the *Shp-2*$^{\Delta 46–110}$ mutation creates a severe loss of function allele. The failure of the Shp-2$^{\Delta 46–110}$ protein to support gastrulation indicates that the mutant Shp-2 protein lacking an intact SH2-N is defective in signalling. Moreover, the remaining SH2-C sequence is not sufficient to direct a stable association of the phosphatase with the PDGFR. The ability to bind upstream phosphotyrosine-containing proteins, such as activated receptors, appears to be crucial for signal transduction by SH2-containing proteins. For example, recent genetic evidence indicates that a point mutation which disrupts the csw binding site in the *Drosophila* Torso RTK phenocopies loss of function *Torso* or *csw* alleles, indicating this receptor–phosphatase interaction is essential for receptor signalling (Cleghon *et al.*, 1996). Here, we find that a mutant Shp-2 protein that lacks a functional SH2-N domain and does not bind to upstream targets is severely compromised in its biological function.

Shp-2 is required for gastrulation and mesoderm formation

Gastrulation is a complex process that involves co-ordination of cell division, differentiation and migration and results in the formation of the third major cell layer, the mesoderm (reviewed in Beddington and Smith, 1993). During gastrulation, several populations of mesoderm are induced, including axial mesoderm (node and notochord), paraxial mesoderm (somites) and extra-embryonic mesoderm (yolk sac and allantoic mesoderm). In homozygous *Shp-2*$^{\Delta 46–110}$ mutant embryos, formation of all these subpopulations was affected to some degree. Most importantly, staining of embryos for *cobl* or *T* expression showed that axial mesoderm was severely perturbed in *Shp-2*$^{\Delta 46–110}$ mutant embryos. Abnormal projections of *cobl*- or *T*-positive cells could be observed, suggesting that Shp-2 is required for proper organization or migration of mesodermal cells during gastrulation.

Some *Shp-2*$^{\Delta 46–110}$ embryos failed to express *cobl* or *T*, and may represent a population of mutants that later failed to develop an A–P axis. These results suggest that Shp-2 may also act at an earlier stage during formation of the node. The defects observed in mutant embryos suggests that the Shp-2 phosphatase acts downstream of one or more receptor (or receptor-linked) tyrosine kinases to control the formation, movement or organization of mesodermal cells. Tyrosine kinase and Ras signal transduction cascades appear to be required for gastrulation to proceed normally; in addition to this study on *Shp-2*, mutations within the *Fgf-R1*, *csk*, *Fak* and the *Gap/Nf1* (double mutant) loci have all been shown to interfere with mesoderm formation (Immamoto and Soriano, 1993; Nada *et al.*, 1993; Deng *et al.*, 1994; Yamaguchi *et al.*, 1994; Furuta *et al.*, 1995; Henkemeyer *et al.*, 1995). For all of these mutations, mutant embryos implant and initiate gastrulation, but subsequently fail to complete this process and die prior to E10.5. Our results indicate that Shp-2 is a critical target of tyrosine kinases during gastrulation, and may act by regulating phosphorylation events that in turn control the Ras/MAP kinase pathway.

Dominant-negative studies of Fgf-R1 and Shp-2 proteins have been performed by micro-injection of mutant RNAs into *Xenopus* embryos (Amaya *et al.*, 1991; Tang *et al.*, 1995). There are similarities and differences between the outcome of these studies compared with results obtained from genetic analysis of mouse mutants. In both species, embryos initiated gastrulation, but did not complete this process normally and exhibited severe posterior truncations, abnormal notochord development and disorganized neural tubes. Although not apparent in the *Xenopus* studies, mutation of either *Shp-2* or *Fgf-R1* in mouse embryos frequently affected the development of anterior structures, including the formation of branchial arches, head mesenchyme and closure of the neuroectoderm. Furthermore, expression of dominant-negative Fgf-R1 or Shp-2 in *Xenopus* led to an apparent reduction in axial mesoderm, whereas the *Fgf-R1* and *Shp-2* mutations in mice often lead to an expansion of axial mesoderm. The molecular reasons for these differences are unclear, however, they may reflect differences between the experimental design of injection of dominant-negative RNAs as compared with targeted gene mutations, or differences in the inherent developmental patterning between *Xenopus* and mice.

Shp-2 modulates RTK signalling

We have used cells derived from homozygous mutant embryos to investigate the role of Shp-2 in the MAP kinase pathway. It has been reported that Shp-2 is required for the induction of DNA synthesis and c-fos transactivation downstream of the PDGFR (Rivard *et al.*, 1995). Conversely, it has also been reported that Shp-2 is not involved in Elk-1 transactivation or S phase entry in response to PDGF (Bennett *et al.*, 1996). The experiments reported here show that activation of MAP kinase in response to PDGF was enhanced in *Shp-2* mutant embryonic cells as compared with their WT counterparts. This is consistent with a model in which the WT Shp-2 protein, via its SH2 domains, is recruited to and subsequently dephosphorylates the activated PDGFR, leading to receptor inactivation and down-regulation of the Ras/MAP kinase cascade. Indeed, phosphotyrosine blots of lysates from PDGF stimulated WT or mutant cells indicated that Shp-2 is involved in down-regulating the phosphotyrosine content of the PDGFR (data not shown). In contrast to its apparent inhibitory role in PDGFR signalling to MAP kinase, functional Shp-2 protein is required for both the initial and sustained activation of MAP kinase in response to FGF. Although the mechanism through which Shp-2 might enhance signalling through the MAP kinase pathway is not known, it is possible that dephosphorylation of

tyrosine sites that engage the SH2 domains of proteins that antagonize the Ras pathway, such as GAP, would contribute in a positive manner to Ras/MAP kinase activation.

A linear signalling pathway has been described (Pawson, 1993), through which a variety of distinct growth factor receptors activate the Ras/MAP kinase cascade. However, these observations do not explain how different receptors utilize this same pathway to induce distinct cellular responses such as proliferation, differentiation or migration. In PC12 cells, the decision to proliferate or differentiate in response to signalling by RTKs is controlled, at least in part, by the potency and duration of MAP kinase activation (Marshall, 1995). Our results suggest that Shp-2 may represent a widely utilized target which modulates the intensity and duration of MAP kinase activation, depending on the nature of the specific receptor that has been stimulated. Therefore, Shp-2 plays a key role downstream of RTKs in defining the specificity of cellular responses to external cues. The profound phenotype of *Shp-2* mutant embryos suggests that the interactions of Shp-2 with receptors, and its role in controlling intracellular signalling, are of biological significance.

Materials and methods

Shp-2 gene targeting

A library of 129/Sv strain mouse genomic DNA was screened with the *Shp-2* cDNA. Positive clones were characterized by restriction mapping and sequence analysis to identify intron–exon structure. A targeting vector was constructed by inserting 1.7 and 5.5 kb fragments from the 5′ end of the *Shp-2* gene into pPNT (Tybulewicz *et al.*, 1991). Genomic sequences were cloned into the vector in the opposite transcriptional orientation to the neo^r cassette. The linearized targeting vector was electroporated into the ES cell line R1 (Nagy *et al.*, 1993) and colonies were isolated following selection in G418 and gancyclovir (Wurst and Joyner, 1993). Double resistant cell clones were expanded and purified genomic DNA was screened for homologous recombination by Southern blotting with the 3′ external probe. Eight out of 200 cell lines screened exhibited a 4.3 kb mutant-specific *Nco*I fragment. Similar blots were also screened with a neo^r probe to check for multiple insertion events (data not shown). Germline transmitting chimeras of three independent *Shp-2*+/– cell lines (8.14, 5.20 and 6.23) were obtained by aggregating ES cells with morula-staged CD1 embryos (Nagy *et al.*, 1993). Subsequent germline mice were analyzed in an inbred (129Sv), mixed (129Sv×CD1) and CD1 (>95%) outbred backgrounds with no observable difference in phenotype.

The *Shp-2* mutation was routinely genotyped using the following oligonucleotides:

Shp-2 E1AS: GTA GGA GCC CTA TAG AAT CTG
PCRneoβ2: TAC CCG GTA GAA TTG ACC TGC AG
Shp-2 10: GAG TCA CAC AGA TCG TAT GCA TCC CA
Shp-2 11: GAT ACG CCT TCT CTC AAT GGA C

Shp-2 E1AS and PCRneoβ2 detect the mutant allele of 250 bp, and Shp-2 10 and Shp-2 11 oligonucleotides amplify the WT allele of 311 bp.

Western blot analysis

E8.0 embryos were lysed in 50 µl (WT) or 25 µl (mutant) TxLB (1% Triton X-100, 138 mM NaCl, 20 mM Tris pH 8.0, 2 mM EDTA, 10% glycerol, plus protease inhibitors). Denatured lysates were resolved on 10% polyacrylamide gels and transferred to Immobilon-P membrane (Millipore). Membranes were blocked in 5% milk powder in TBST (0.05% Tween-20) and Western blots were performed with either anti-Shp-2 SH2 (Feng *et al.*, 1993), anti-GAP (UBI) or anti-Shp-2 C-terminus (Santa Cruz) polyclonal antibodies, followed by protein A–HRP (Bio-Rad) and chemiluminesence. Immunoblotting was analyzed with a Molecular Dynamics computing densitometer (model 300A).

Marker analysis

For β-galactosidase staining, male mice compound heterozygous for the *Shp-2* mutation and a LacZ (*cobl*-, *Flk1- or Nuk*-) marker were mated to *Shp-2* heterozygous females. In the course of crossing the *Shp-2* and *Flk1* mutations, a genetic linkage between these two loci was identified with a recombination frequency of 0.032. Collection, X-gal staining, sectioning and photography was performed as described (Henkemeyer *et al.*, 1996). Whole-mount *in situ* hybridization was performed as described (Conlon and Rossant, 1992).

Establishing cell lines

E9.5 embryos were dissected and, due to the decreased cell number in *Shp-2*$^{\Delta 46-110}$ mutants as compared with WT embryos, mutant embryos from each litter were pooled in order to plate approximately the same cell numbers as for the WT cultures. Single cell suspensions were prepared by treatment with 0.1% trypsin for 2–5 min. Cells were plated in DMEM, 15% FCS, 5% embryo fibroblast conditioned medium. Genotyping of the cell lines was performed by PCR and Western blotting analysis. All experiments were performed on cells between passage 5 and 9, prior to crisis, by comparing cell cultures from either littermates or equivalent passage number. PDGF and FGF time courses were performed a minimum of three times on two independent cell lines of each genotype, and representative results are shown.

Growth factor stimulations of cell cultures, analysis of phosphotyrosine induction and MAP kinase gel mobility

The GST fusion of the tandem SH2 domains with the internal deletion of amino acids 46–110 was cloned by amplification of the mutant mRNA from heterozygous cells. The PCR product was cloned into pGEX4T-2 and sequenced on both strands with the ALF automated DNA sequencer (Pharmacia). Sequence analysis revealed that amino acid 46 of the Shp-2Δ protein is encoded by a chimeric codon generated by in frame splicing between codons 46 and 111. The WT GST-SH2 N+C, expression and purification has been previously described (Feng *et al.*, 1993). Embryo fibroblasts or NIH 3T3 cells were grown to sub-confluency, serum starved for 48 h and stimulated for the times indicated with 100 ng/ml PDGF-BB (UBI). For immunoprecipitations (IPs) or GST mixing experiments, cells were lysed in TxLB, protein concentrations determined by bicinchoninic acid assay (Pierce) and equal amounts of lysate were precipitated with anti-Shp-2 antibody or 2 µg of GST fusion. IPs/mixes were washed three times in TxLB and were eluted from the beads by boiling for 5 min in 1× sample buffer and proteins were resolved on 10% acrylamide gels. Membranes were blocked in 1% gelatin and probed with anti-phosphotyrosine 4G10 (UBI). Goat anti-mouse–HRP (Bio-Rad) was utilized as the secondary reagent. Embryo fibroblast cells were grown to sub-confluency and serum starved for 70 h. For FGF stimulations, a media change into DMEM + 1 µg/ml heparin was performed prior to cell stimulations. Cells were then stimulated with a mixture of both acidic and basic FGF (Promega and UBI; final concentration 100 ng/ml). Cells were lysed in 1× sample buffer, boiled, DNA was sheared and proteins were resolved on 12% acrylamide: 0.12% bisacrylamide gels and Western blotted with anti-MAP kinase monoclonal antibody (UBI).

Acknowledgements

We thank K.Harpal for help with histology, V.K.Lai for help with establishing cell lines, A.Cheng for help with gene targeting, D.Hu for help with sequencing, S.Holland for critical review of the manuscript and J.Rossant for many invaluable discussions. Predoctoral support for T.M.S. and postdoctoral support for M.H. was from the Medical Research Council of Canada. G.S.F. has a career development award from the American Diabetes Association. This work was supported by grants from Bristol Myers Squibb and the MRC, a Terry Fox programme grant from the National Cancer Institute of Canada (NCIC) and a Howard Hughes International Research Scholar Award to T.P. T.P. is a Terry Fox Cancer Research Scientist of the NCIC.

References

Adachi,M., Fischer,E.H., Ihle,J., Imai,K., Jirik,F., Neel,B., Pawson,T., Shen,S.-H., Thomas,M., Ullrich,A. and Zhao,Z. (1996) Mammalian SH2-containing protein tyrosine phosphatases. *Cell*, **85**, 15.

Ahmad,M., Sekiya,M., Miyachi,T., Matsuno,K. and Hinoda,Y. (1993) A widely expressed human protein-tyrosine phosphatase containing src homology 2 domains. *Proc. Natl Acad. Sci. USA*, **90**, 2197–2201.

Allard,J.D., Chang,H.C., Herbst,R., McNeill,H. and Simon,M.,A. (1996) The SH2-containing tyrosine phosphatase Corkscrew is required during signalling by Sevenless, Ras1 and Raf. *Development*, **122**, 1137–1146.

Amaya,E., Musci,T.J. and Kirschner,M.W. (1991) Expression of a dominant negative mutant of the FGF receptor disrupts mesoderm formation in *Xenopus* embryos. *Cell*, **66**, 257–270.

Arrandale,J.M., Gore-Willse,A., Rocks,S., Ren,J.-M., Zhu,J., Davis,A., Livingston,J.N. and Rabin,D.U. (1996) Insulin signalling in mice expressing reduced levels of Syp. *J. Biol. Chem.*, **271**, 21353–21358.

Beddington,R.S.P. and Smith,J.C. (1993) Control of vertebrate gastrulation: inducing signals and responding genes. *Curr. Opin. Genet. Dev.*, **3**, 655–661.

Bennett,A.M., Tang,T.L., Sugimoto,S., Walsh,C.T. and Neel,B.G. (1994) Protein-tyrosine-phosphatase SH-PTP2 couples PDGF-receptor to ras. *Proc. Natl Acad. Sci. USA*, **91**, 7335–7339.

Bennett,A.M., Hausdorff,S.F., O'Reilly,A.M., Freeman,R.M. and Neel,B.G. (1996) Multiple requirements for SH-PTP2 in epidermal growth factor mediated cell cycle progression. *Mol. Cell. Biol.*, **16**, 1189–1202.

Case,R.D., Piccione,E., Wolf,G., Bennett,A.M., Lechleider,R.J., Neel,B.G. and Shoelson,S.E. (1994) SH-PTP2/Syp SH2 domain binding specificity is defined by direct interactions with platelet-derived growth factor beta-receptor, epidermal growth factor receptor and insulin receptor substrate-1-derived phosphopeptides. *J. Biol. Chem.*, **269**, 10467–10474.

Cleghon,V., Gayko,U., Copeland,T.D., Perkins,L.A., Perrimon,N. and Morrison,D.K. (1996) *Drosophila* terminal structure development is regulated by compensatory activities of positive and negative phosphotyrosine signalling sites on the Torso RTK. *Genes Dev.*, **10**, 566–577.

Cohen,G.B., Ren,R. and Baltimore,D. (1995) Modular binding domains in signal transduction proteins. *Cell*, **80**, 237–248.

Conlon,R.A. and Rossant,J. (1992) Exogenous retinoic acid rapidly induces anterior ectopic expression of murine Hox-2 genes *in vivo*. *Development*, **116**, 357–368.

Cooper,J.A. and Howell,B. (1993) The when and how of Src regulation. *Cell*, **73**, 1051–1054.

Cyster,J.G. and Goodnow,C.C. (1995) Protein tyrosine phosphatase 1C negatively regulates antigen receptor signalling in B lymphocytes and determines thresholds for negative selection. *Immunity*, **2**, 1–12.

D'Ambrosio,D., Hippen,K.L., Minskoff,S.A., Mellman,I., Pani,G., Siminovitch,K. and Cambier,J.C. (1995) Recruitment and activation of PTP1C in negative regulation of antigen receptor signalling by FcγR1. *Science*, **268**, 293–296.

Deng,C., Wynshaw-Boris,A., Shen,M.M., Daugherty,C., Ornitz,D.M. and Leder,P. (1994) Murine FGFR-1 is required for early postimplantation growth and axial formation. *Genes Dev.*, **8**, 3045–3057.

Eck,M., Pluskey,S., Trub,T., Harrison,S.C. and Shoelson,S.E. (1996) Spatial constraints on the recognition of phosphoproteins by the tandem SH2 domains of the phosphatase SH-PTP2. *Nature*, **379**, 277–280.

Feng,G., Hui,C. and Pawson,T. (1993) SH2-containing phosphotyrosine phosphatase as a target of protein-tyrosine kinases. *Science*, **259**, 1607–1611.

Feng,G., Shen,R., Heng,H.H.-Q., Tsui,L.-C., Kazlauskas,A. and Pawson,T. (1994) Receptor-binding, tyrosine phosphorylation and chromosome localization of the mouse SH2-containing phospho-tyrosine phosphatase Syp. *Oncogene*, **9**, 1545–1550.

Freeman,R.M., Plutzky,J. and Neel,B.G. (1992) Identification of a human src homology 2-containing protein-tyrosine-phosphatase: A putative homolog of *Drosophila* corkscrew. *Proc. Natl Acad. Sci. USA*, **89**, 11239–11243.

Furuta,Y., Ilic,D., Kanazawa,S., Takeda,N., Yamamoto,T. and Aizawa,S. (1995) Mesodermal defect in late phase of gastrulation by a targeted mutation of focal adhesion kinase, FAK. *Oncogene*, **11**, 1989–1995.

Gasca,S., Hill,D.P., Klingensmith,J. and Rossant,J. (1995) Characterization of a gene trap insertion into a novel gene, *Cordon-bleu*, expressed in axial structures of the gastrulating mouse embryo. *Dev. Genet.*, **17**, 141–154.

Gotoh,Y., Masuyama,N., Suzuki,A., Ueno.N. and Nishida,E. (1995) Involvement of the MAP kinase cascade in *Xenopus* mesoderm induction. *EMBO J.*, **14**, 2491–2498.

Henkemeyer,M., Rossi,D.J., Holmyard,D.P., Puri,M.C., Mbamalu,G., Harpal,K., Shih,T.S., Jacks,T. and Pawson,T. (1995) Vascular system defects and neuronal apoptosis in mice lacking Ras GTPase-activating protein. *Nature*, **377**, 695–701.

Henkemeyer,M., Orioli,D., Henderson,J.T., Saxton,T.M., Roder,J., Pawson,T. and Klein,R. (1996) Nuk controls pathfinding of commissural axons in the mammalian central nervous system. *Cell*, **86**, 35–46.

Herbst,R., Carroll,P.M., Allard,J.D., Schilling,J., Raabe,T. and Simon, M.A. (1996) Daughter of sevenless is a substrate of the phosphotyrosine phosphatase corkscrew and functions during sevenless signalling. *Cell*, **85**, 911–920.

Hunter,T. (1995) Protein kinases and phosphatases: the Yin and Yang of protein phosphorylation and signaling. *Cell*, **80**, 225–236.

Immamoto,A. and Soriano,P. (1993) Disruption of the *csk* gene, encoding a negative regulator of src family tyrosine kinases, leads to neural tube defects and embryonic lethality in mice. *Cell*, **73**, 1117–1124.

Kazlauskas,A., Feng,G., Pawson,T. and Valius,M. (1993) The 64kd protein that associates with the PDGFR β subunit via tyrosine 1009 is the SH2-containing phosphotyrosine phosphatase Syp. *Proc. Natl Acad. Sci. USA*, **90**, 6939–6943.

Klingmuller,U., Lorenz,U., Cantley,L.C., Neel,B.G. and Lodish,H.F. (1995) Specific recruitment of SH-PTP1 to the erythropoietin receptor causes inactivation of JAK2 and termination of proliferative signals. *Cell*, **80**, 729–738.

LaBonne,C., Burke,B. and Whitman,W. (1995) Role of MAP kinase in mesoderm induction and axial patterning during *Xenopus* development. *Development*, **121**, 1475–1486.

Lechleider,R.J., Sugimoto,S., Bennett,A.M., Kashishian,A.S., Cooper, J.A., Shoelson,S.E., Walsh,C.T. and Neel,B.G. (1993a) Activation of the SH2-containing phosphotyrosine phosphatase SH-PTP2 by its binding site, phosphotyrosine 1009, on the human PDGF-R β. *J. Biol. Chem.*, **268**, 21478–21481.

Lechleider,R.J., Freeman,R.M. and Neel,B.G. (1993b) Tyrosyl phosphorylation and growth factor receptor association of human *corkscrew* homologue, SH-PTP2. *J. Biol. Chem.*, **268**, 13434–13438.

Lee,C., Kominos,D., Jacques,S., Margolis,B., Schlessinger,J., Shoelson,S.E. and Kuriyan,J. (1994) Crystal structures of peptide complexes of the amino-terminal SH2 domain of the Syp tyrosine phosphatase. *Structure*, **2**, 423–438.

Li,W., Nishimura,R., Kashishian,A., Batzer,A.G., Kim,W.J., Cooper,J. and Schlessinger,J. (1994) A new function for a phosphotyrosine phosphatase: Linking Grb2-Sos to a receptor tyrosine kinase. *Mol. Cell. Biol.*, **14**, 509–517.

Marengere,L.E.M., Waterhouse,P., Duncan,G.S., Mittrucker,H.-W., Feng,G.-S. and Mak,T.W. (1996) Regulation of T cell receptor signaling by tyrosine phosphatase SYP association with CTLA-4. *Science*, **272**, 1170–1173.

Milarski,K.L. and Saltiel,A.R. (1994) Expression of catalytically inactive Syp phosphatase in 3T3 cells blocks stimulation of MAP kinase by insulin. *J. Biol. Chem.*, **269**, 21239–21243.

Marshall,C.J. (1995) Specificity of receptor tyrosine kinase signaling: transient versus sustained extracellular signal-regulated kinase activation. *Cell*, **80**, 179–185.

Nada,S., Yagi,T.T.H., Tokunaga,T., Nakagawa,H., Ikawa,Y., Okada,M. and Aizawa,S. (1993) Constitutive activation of Src family kinases in mouse embryos that lack Csk. *Cell*, **73**, 1125–1135.

Nagy,A., Rossant,J., Nagy,R., Abramow-Newerly,W. and Roder,J.C. (1993) Derivation of completely cell culture derived mice from early-passage embryonic stem cells. *Proc. Natl Acad. Sci. USA.*, **90**, 8424–8428.

Noguchi,T., Matozaki,T., Horita,K., Fujioka,Y. and Kasuga,M. (1994) Role of SH-PTP2, a protein-tyrosine phophatase with Src homology 2 domains, in Insulin stimulated Ras activation. *Mol. Cell. Biol.*, **14**, 6674–6682.

Paulson,R.F., Vesely,S., Siminovitch,K.A. and Bernstein,A. (1996) Signaling by the *W/Kit* receptor tyrosine kinase is negatively regulated *in vivo* by the protein tyrosine phosphatase PTP1C. *Nature Genet.* **13**, 309–315.

Pawson,T. (1993) Signal transduction-A conserved pathway from the membrane to the nucleus. *Dev. Genet.*, **14**, 333–338.

Pawson,T. (1995) Protein modules and signalling networks. *Nature*, **373**, 573–579.

Pei,D., Wang,J. and Walsh,C.T. (1996) Differential functions of the two Src homology 2 domains in protein-tyrosine phosphatase SH-PTP1. *Proc. Natl Acad. Sci. USA*, **93**, 1141–1145.

Perkins,L.A., Larsen,I. and Perrimon,N. (1992) Corkscrew encodes a putative protein tyrosine phosphatase that functions to transduce the terminal signal from the receptor tyrosine kinase torso. *Cell*, **70**, 225–236.

Pluskey,S., Wandlass,T.J., Walsh,C.T. and Shoelson,S.E. (1995) Potent stimulation of SH-PTP2 phosphatase activity by simultaneous occupancy of both SH2 domains. *J. Biol. Chem.*, **270**, 2897–2900.

Raabe,T., Riesgo-Escover,J., Liu,X., Bausenwien,B.S., Deak,P., Maroy,P. and Hafen,E. (1996) DOS, a novel pleckstrin homology domain-containing protein required for signal transduction between sevenless and Ras1 in *Drosophila*. *Cell*, **85**, 911–920.

Rivard,N., McKenzie,F.R., Brondello,J. and Pouyssegur,J. (1995) The phosphotyrosine phosphatase PTP1D, but not PTP1C, is an essential mediator of fibroblast proliferation induced by tyrosine kinase and G protein-coupled receptors. *J. Biol. Chem.*, **270**, 11017–11024.

Shalaby,F., Rossant,J., Yamaguchi,T.P., Breitman,M.L. and Schuh,A.C. (1995) Failure of blood-island formation and vasculogenesis in Flk-1-deficient mice. *Nature*, **376**, 62–66.

Shultz,L.D., Schweitzer,P.A., Rajan,T.V., Yi,T., Ihle,J.N., Matthews,R.J., Thomas,M.L. and Beier,D.R. (1993) Mutations at the murine motheaten locus are within the hematopoietic cell protein-tyrosine phosphatase gene. *Cell*, **73**, 1445–1454.

Simon,M.A., Bowtell,D.D.L., Dodson,G.S., Laverty,T.R. and Rubin,G.M. (1991) Ras1 and a putative guanine nucleotide exchange factor perform crucial steps in signalling by the Sevenless protein tyrosine kinase. *Cell*, **67**, 701–716.

Songyang,Z. *et al.* (1994) Specific motifs recognized by the SH2 domains of Csk, 3BP2, fps/fes, Grb2, HCP, SHC, Syk and Vav. *Mol. Cell. Biol.*, **14**, 2777–2785.

Sun,H. and Tonks,N.K. (1994) The coordinated action of protein tyrosine phosphatases and kinases in cell signaling. *Trends Biochem. Sci.*, **19**, 480–485.

Tang,T.L., Freeman,R.M., O'Reilly,A.M., Neel,B.G. and Sokol,S.Y. (1995) The SH2-containing protein-tyrosine phosphatase SH-PTP2 is required upstream of MAP kinase for early *Xenopus* development. *Cell*, **80**, 473–483.

Tsui,H.W., Siminovitch,K.A., de Souza,L. and Tsui,F.W.L. (1993) *Motheaten* and *viable motheaten* mice have mutations in the haematopoietic cell phosphatase gene. *Nature Genet.*, **4**, 124–129.

Tybulewicz,V.L.J., Crawford,C.E., Jackson,P.K., Bronson,R.T. and Mulligan,R.C. (1991) Neonatal lethality and lymphopenia in mice with a homozygous disruption of the c-abl proto-oncogene. *Cell*, **65**, 1153–1163.

Umbhauer,M., Marshall,C., Mason,C.S., Old,R.W. and Smith,J.C. (1995) Mesoderm induction in *Xenopus* caused by activation of MAP kinase. *Nature*, **376**, 58–62.

Vogel,W., Lammers,R., Huang,J. and Ullrich,A. (1993) Activation of a phosphotyrosine phosphatase by tyrosine phosphorylation. *Science*, **259**, 1611–1613.

Welham,M.J., Dechert,U., Jirik,F. and Schrader,J.W. (1994) Interleukin (IL)-3 and GM-CSF, but not IL-4, induce tyrosine phosphorylation, activation, and association of SH-PTP2 with Grb2 and PI3-Kinase. *J. Biol. Chem.*, **269**, 23764–23768.

Wilkinson,D.G., Bhatt,S. and Herrmann,B.G. (1990) Expression pattern of the mouse *T* gene and its role in mesoderm formation. *Nature*, **343**, 657–659.

Wurst,W. and Joyner,A.L. (1993) *Gene Targeting: A Practical Approach*. Oxford University Press, Oxford, UK, pp. 31–62.

Yamaguchi,T.P., Harpal,K., Henkemeyer,M. and Rossant,J. (1994) Fgfr-1 is required for embryonic growth and mesodermal patterning during mouse gastrulation. *Genes Dev.*, **8**, 3032–3044.

Yi,T., Mui,A.L., Krystal,G. and Ihle,J.N. (1993) Hematopoietic Cell Phosphatase associates with the Interleukin-3 receptor β chain and down-regulates IL-3 induced tyrosine phosphorylation and mitogenesis. *Mol. Cell. Biol.*, **13**, 7577–7586.

Received on October 2, 1996; revised on December 19, 1996